

The Effect of Geosynthetic Reinforcement on the Damage Propagation Rate of Asphalt Pavements

H.R.A. Hosseini¹, A.K. Darban^{2,*} and K. Fakhri³

Abstract. *There are several approaches for modeling the fatigue life and damage of asphalt pavements, such as stress-strain and damage mechanics. In this research, a simple mechanistic approach is used to explain the destruction of asphalt pavements. For asphalt reinforcement, two types of geosynthetic were used in the airfield at Imam Khomeini airport, Tehran. Non-reinforced, reinforced with a geogrid and geotextile specimens with dimensions of 50 × 63 × 381 mm were obtained from the asphalt slab field section. Fatigue tests of this study have been conducted with a four point beam test and a fatigue load with a half-sin wave at a frequency of 10 cycle/sec (no rest period), has been used. The results indicated that specimens reinforced with geosynthetics exhibit a higher initial stiffness module and lower crack propagation rate than non-reinforced specimens.*

Keywords: *Asphalt pavement; Failure; Geosynthetics; Geogrid; Geotextile; Beam fatigue test crack propagation.*

INTRODUCTION

The creation of cracks due to loading is one of the most important causes of damage in asphalt pavements [1]. These cracks are developed as fatigue cracks (top to bottom and reverse), longitudinal cracks and transverse cracks. Increased maintenance and rehabilitation of airfields and highways are going to be one of the most critical problems. Now, airport and highway agencies are being pressured to maintain a level of service to highways and airfield users with decreasing budgets [2,3].

Geosynthetics are a group of polymeric materials which are applied more and more in engineering projects, such as road and airport construction [4,5]. Research shows that the use of geosynthetics can effectively prevent the propagation of cracks and, therefore, the propagation of damage to pavements [6,7].

Geosynthetics are divided into five general groups: Geotextiles, Geogrids, Geonets, Geomembranes and

Geocomposites. These products have high tensile strength and could effectively reinforce materials which are weak in tension. Hence, employing layers of geosynthetics in soil or asphalt, which are characteristically weak in tension, could improve their tensile strength. The mass of reinforced soil or asphalt is considered to have a better load carrying capacity and higher tensile strength than non-reinforced soil or asphalt [8-10].

Geotextiles, geogrids and geocomposites are types of geosynthetic commonly used in soil or asphalt pavements as reinforcing agents [11,12]. Geosynthetics are usually employed in asphalt pavements for such functions as reinforcement, separation, drainage and water proofing layers. Studies conducted over the last 20 years have mainly concentrated on the advantages of geosynthetics when applied with, or under, non-cohesive layers [13,14]. The advantages of such materials are generally stated in the Traffic Benefit Ratio (TBR), which indicates the increase in service life of reinforced pavements compared to non-reinforced ones. Also, there is a sub-base thickness reduction ratio (BCR), which indicates the reduction in sub-base thickness for non-reinforced pavements [15,16]. A geosynthetic layer, especially a geotextile layer, is used beneath asphalt overlays, ranging in thickness from 25 to 100 mm of Asphalt Concrete (AC) or Portland Cement Concrete (PCC). The geotextile layer is generally combined with asphalt sealant, or tack coat, to form a membrane interlayer system, known as a

1. Faculty of Engineering, Kurdistan University, P.O. Box 416, Sanandaj, Iran.

2. Department of Engineering, Tarbiat Modares University, P.O. Box 4115-143, Tehran, Iran.

3. Department of Civil and Environmental Engineering, Khaje-Nasiradin-Toosi University, P.O. Box 1996715433, Tehran, Iran.

*. Corresponding author. E-mail: akdarban@modares.ac.ir

Received 24 June 2006; received in revised form 26 August 2007; accepted 17 May 2008

paving fabric interlayer [17]. When properly installed, a geotextile layer beneath the asphalt overlay mainly functions as:

- Fluid barrier (if impregnated with bitumen, that is, asphalt cement), protecting the underlying layers from degradation due to the infiltration of road-surface moisture;
- Cushion, that is, a stress-relieving layer for the overlays; retarding and controlling some common types of cracking, including reflective cracking.

The use of fabrics in asphalt paving systems began in 1966. Still, there is no clear understanding of the effect of geosynthetics on asphalt performance. Since that time, their performance has been monitored and evaluated to provide a basis for better design and installation procedures [4,5]. The geosynthetics used in asphalt reinforcement are commonly geotextile and geogride. A paving geosynthetic system consists of a geosynthetic which is installed in the asphalt layer. To date, both laboratory simulations and large-scale field trials have been used to evaluate potential overlay reinforcement systems.

There are a wide range of approaches in modeling the fatigue and destruction of asphalt mixes, from simple stress-strain methods to complicated approaches such as damage mechanics. TMU (Tarbiat Modares University) has recently completed an effort to quantify the stiffness, fatigue characteristics and crack propagation of asphalt reinforcement geosynthetics, using modified index tests and a beam flexure test.

Theory of Crack

Traditionally, fatigue is divided into two stages; crack initiation and crack propagation. Crack initiation has been defined as the growth and coalescence of micro cracks. Crack propagation has been defined as the growth of macro cracks.

Results of laboratory fatigue tests and full scale field studies indicate that the effective stiffness modulus of asphaltic materials is reduced significantly under repeated loading without the presence of visible cracks. This indicates that damage is accumulating in the material, thus, reducing the effective volume able to carry applied loads (in other words, the effective stiffness modulus is reduced).

Continuum damage mechanics evolved in the 1960s as a way of representing the collective effect of crack-like defects on deterioration under mechanical loading.

The state of the material is often reported by using a scalar variable, varying between 0 (undamaged) to 1 (fully damaged) [17,18].

From damage mechanic concepts, the internal damage to a body can be expressed in terms of a

reduction in the effective area under uniaxial loading:

$$D = \frac{A_D}{A}, \quad (1)$$

where A_D = Area of the cracked surface and A = total area.

It is clear that D is varying between 0 and 1. Lemaitre [17] mentioned that the above equation should be expressed by the use of the elastic modulus (Young's) for pavement engineering applications. Therefore, Equation 1 can be used applying the following stiffness modulus [10]:

$$D = \frac{S - S_e}{S}, \quad (2)$$

where S_e is the effective stiffness modulus and S is the intact material modulus.

It is assumed that damage gradually increases as the number of loading cycles increase. The rate of damage growth per cycle can be expressed as a function of critical parameters, which represent the material characteristics and test conditions as follows:

$$\frac{dD}{dN} = f(\sigma, \varepsilon, T, \dots), \quad (3)$$

where σ is stress, ε is strain and T is temperature.

Using data from fatigue tests, function f for one dimensional conditions can be developed.

If $\frac{dD}{dN}$ is to be plotted against the initial strain in the logarithmic scale, a straight line may be drawn with the following general equation:

$$\frac{dD}{dN} = B\varepsilon_0^m, \quad (4)$$

where ε_0 is initial strain and B and m are constants (which depend on the characteristics of the asphalt mix) [18].

MATERIALS AND TEST METHOD

To investigate the actual effects of geosynthetic applications on the fatigue life of pavements and for damage propagation rate comparison, sections reinforced with and without geotextile and geogrid employment were constructed in Imam Khomeini Airport.

Materials

The grading of the materials used in this study is shown in Table 1 and the properties of the asphalt mix used in this study are shown in Table 2.

The geotextile used in this study is a polyfelt-PGM14, which is produced for asphalt and which is resistant to heat up to 160 degrees centigrade.

Table 1. The grading of the asphalt constructed on site.

Sieve Size	Percent Passing	Average Range of Specification No.4, Tables 3-18, Publication 101 [19]
3/4 inch	100	100
1/2 inch	95	90-100
3/8 inch	87	-
No. 4	64.5	44-74
No. 8	37.7	28-58
No. 50	10	7-23
No. 200	5	2-10

Table 2. Properties of asphalt mix.

Property	Unit	Value
Percent of Bitumen	%	5.3
Air Voids	%	4.1
Marshal Stability	kg	957
Unit Weight	gr/cm ³	2.21
Field Compaction	%	99

Technical specification of this geotextile, which is stated by the producing company, is shown in Table 3. This type of geotextile is currently being used in the Tehran-Qom highway.

The geogrid used in this study is a mesh type, which was imported by Iran Bana Arian Company. This type of geogrid is also exclusively made for asphalt and is resistant to heat up to 190 degrees centigrade. The geogrid specifications, according to the producing company, are shown in Table 4. This type of geogrid is currently being used in Imam Khomeini Airport as

the local pavement reinforcement.

After the construction of three sections in one of the access roads to Imam Khomeini Airport, a couple of 50×50 cm slabs were taken from each section and were carried to the Central Technical and Soil Mechanics Laboratory of the Ministry of Road and Transportation. A $381 \times 63 \times 50 \pm 5$ mm specimen of the asphalt beams were cut out of the asphalt slab using proper cutters. The specimens were cut with 6 faces and the reinforcing layer was placed 1/3 from the bottom of the specimens [20] (Figure 1).

Beam Flexural Test Method

A beam flexural test may be performed under both stress controlled and strain controlled conditions. The

**Figure 1.** A few prepared specimens.**Table 3.** Properties of the used geotextiles.

Property	Standard	Unit	Value
Product Type	Non woven with bonded fabric		
Raw Material	100% polypropylene, UV stabilized		
Bitumen Retention	ASTM D6140-97	Kg/m ²	101
Tensile Strength	EN ISO 10319	KN/m	9
Elongation at Maximum Load		%	> 55
Grab Tensile Strength	ASTM D4632	N	520
Grab Elongation		%	> 50
Thickness at 2 KN/M ² Load	EN 964-1	mm	104
Mass Per Unit Area	EN 965	g/m ²	140
Coefficient of Variation		%	< 10
Melting Point	ASTM D 276	°C	165
Recycle	100% recyclable by traditional methods		

load is applied in sine waves for stress controlled and sine and a half waves for a strain controlled condition.

For the stress controlled test, the determined stress is applied until the sample breaks. For the strain controlled test, a feedback system is designed to correct the stress after each load cycle, so that the strain remains constant at the determined value.

Introducing Beams Fatigue Testing Apparatus

A beam flexural apparatus was used for determination of the fatigue and crack propagation rate. The photograph of the specimen set up is shown in Figure 2. The apparatus can be employed for flexural load cycles to the asphalt specimens under both stress controlled

and strain controlled conditions. For strain controlled conditions, the measured deflection is corrected in each cycle load, so that the strain can be measured for the next cycle. In stress controlled cases, the deflections are recorded, assuming that the applied force is constant. If creep occurs in the specimens, the maximum and minimum load quantity is corrected to keep the beams straight.

Several parameters are calculated from the test data, including loading period, number of load cycles, maximum and minimum beam deflection, tensile stress and strain and flexural stiffness modulus. For this research, a strain controlled condition was applied to the beam specimen.

Test Setup

The specimens were cut from the slabs and, taking into account the number of required specimens for drawing the fatigue curves, 12 (3 specimens at each level and under 4 different strain levels) specimens were prepared for both reinforced and non-reinforced conditions.

Since the specimens were reinforced at one side and for an improved simulation of crack development, a half sinusoidal loading, at a frequency of 10 HZ, was applied. The specimens were tested at four strain levels. These levels included 700, 900, 1100 and 1300 microns (micro strain) at a temperature of $20 \pm 0.8^\circ\text{C}$. Tests were continued to the beginning of the third stage of stiffness modulus reduction curves versus load cycles.

Figure 3 shows a typical stiffness curve plotted versus the number of loads in a fatigue test under constant strain conditions. The curve can be divided into 3 approximate stages:

Stage 1 This stage is characterized by the rapid reduction of the stiffness modulus and only accounts for approximately 10% of the total fatigue life;

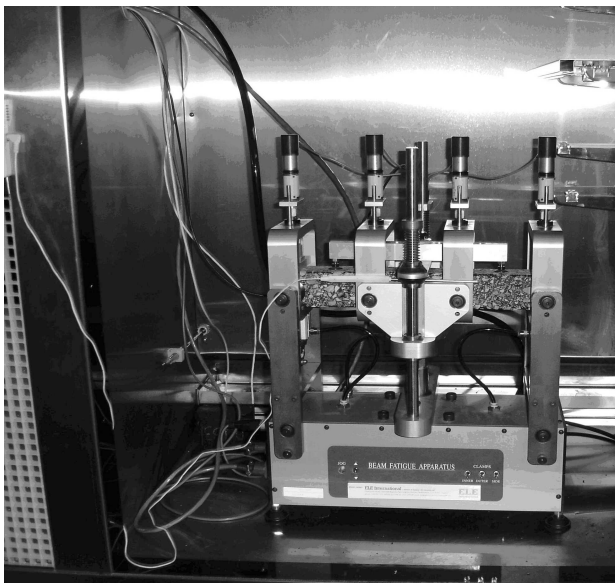


Figure 2. Beam flexural test apparatus setup.

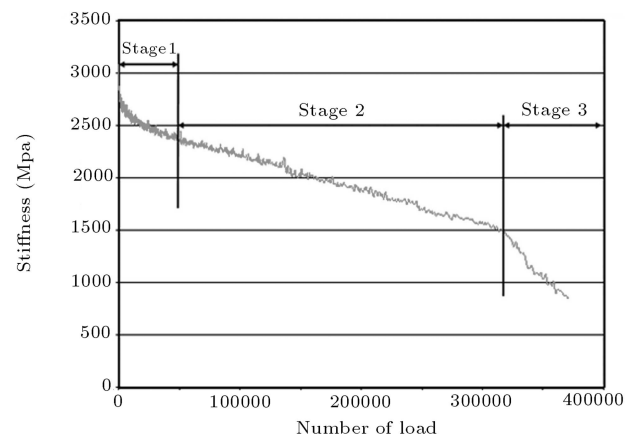


Figure 3. A typical stiffness curve plotted versus the number of loads.

Stage 2 This stage is characterized by an approximate linear reduction in the width number of the loading cycles, representing the stiffness modulus of the specimens.

This part accounts for 90% of the total fatigue life and is the stage where the micro cracks are initiated. This paper focuses mostly on this stage;

Stage 3 The characteristic of this stage is a sudden decrease in the stiffness modulus as the specimen approaches failure. At this stage, macro cracks are developed and, somehow, the beginning of this stage can be considered the end of the fatigue life of the specimen.

RESULTS AND DISCUSSIONS

For the analysis of the crack propagation of the specimen, a damage mechanics approach was used. As already stated, Stage 2 can be characterized by an, approximately, linear relationship between the stiffness modulus reduction and the number of load cycles. This implies that, during this period, the rate of damage accumulation is, approximately, constant. Consequently, a straight line was fitted to the different specimen data with different strain levels at this stage (Figure 3). The imaginary point was the extrapolated fitted line that crosses the stiffness modulus axis, which is defined as the imaginary initial stiffness modulus and denoted as S_0 . The slope of this fitted line has been used to calculate the constant rate of damage accumulation ($\frac{dD}{dN}$). The constant rates of the different specimen damage propagation rates are given in Table 5.

Ultimately, for both conditions, strain level versus ($\frac{dD}{dN}$) was drawn and these points fitted using exponen-

tial regression. These graphs are shown in Figures 4 to 6 and Table 6. According to what has been stated in the introduction and in Equation 4, the factors of B and m , for the three different conditions, are given in Table 7.

As demonstrated in the specimen's stiffness modulus graphs versus load cycle, it is clear that the reinforced specimens have a higher stiffness modulus in comparison to non-reinforced specimens; this dif-

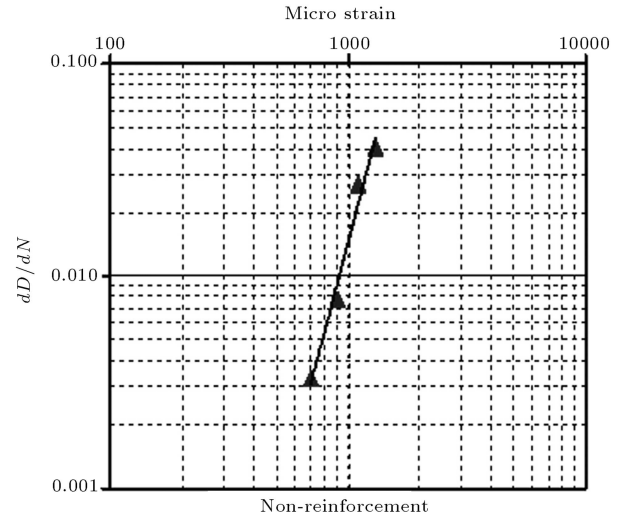


Figure 4. Applied strain level versus damage development rate for non-reinforced specimens.

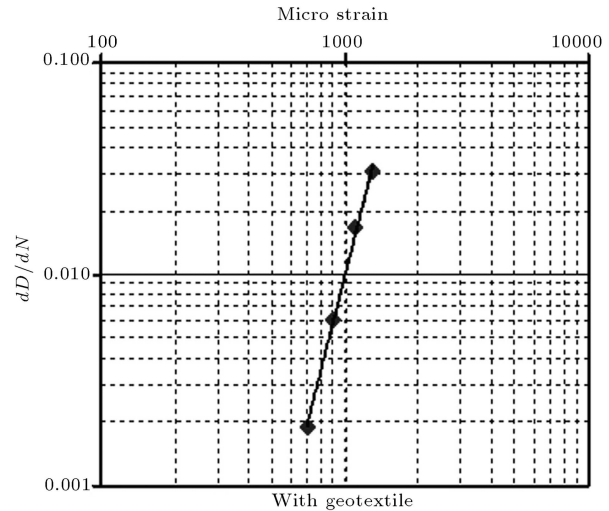


Figure 5. Applied strain level versus damage development rate for reinforced specimens with geotextile.

Table 5. Damage propagation factor in reinforced and non-reinforced specimens for different strain levels ($\frac{dD}{dN}$) (average of three specimens)

Strain Level	Non-reinforced	Reinforced with Geotextile	Reinforced with Geogrid
700	0.0033	0.0019	0.0024
900	0.0077	0.0061	0.0061
1100	0.0271	0.0166	0.0218
1300	0.0402	0.0305	0.0284

Table 6. Fatigue equations according to Equation 4 for different specimens.

Asphalt Specimen	Fatigue Equation	Correlation Factor (R^2)
Non-reinforced	$\frac{dD}{dN} = 2.3918 \times 10^{-15} (\varepsilon)^{4.2600}$	$= 0.9765 R^2$
Reinforced with Geogrid	$\frac{dD}{dN} = 1.9872 \times 10^{-15} (\varepsilon)^{4.2464}$	$= 0.9684 R^2$
Reinforced with Geotextile	$\frac{dD}{dN} = 2.2134 \times 10^{-16} (\varepsilon)^{4.5495}$	$= 0.9972 R^2$

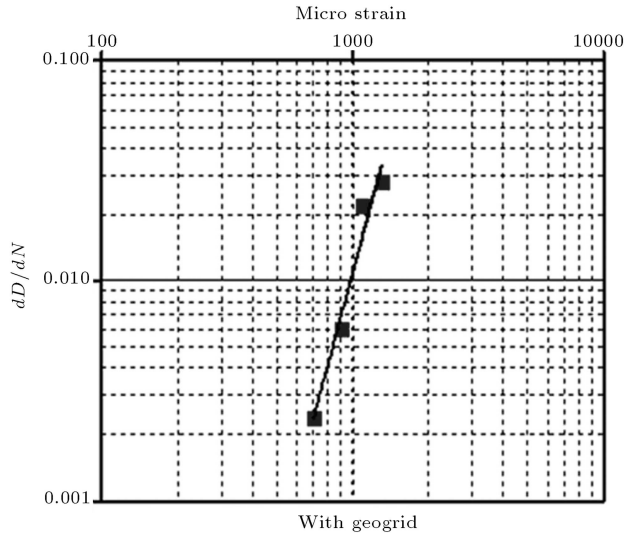


Figure 6. Applied strain level versus damage development rate for reinforced specimens with geogrid.

Table 7. Values of B and m in Equation 4 for different specimens.

Explanations	B	m
Non-reinforced Specimen	6.0867×10^{-15}	4.2600
Reinforced Specimen with Geotextile	2.2134×10^{-16}	4.5495
Reinforced Specimen with Geogrid	1.9872×10^{-15}	4.2464

ference is even higher for specimens reinforced with geogrids. The experimental results are agreement with the findings of Saraf et al. [2]. Figures 7 and 8 show that fatigue versus damage propagation rate lines is moving towards the bottom of the graphs for the non-reinforced condition. The calculated values of B in Table 7 indicate that the rate of damage propagation in reinforced specimens is lower than that for the non-reinforced specimens.

CONCLUSION

This research indicated that specimens reinforced with geosynthetics have improved stability and integrity compared to non-reinforced specimens. Moreover, the widths of the cracks are decreased. This is because, at the end of the reinforced specimens fatigue life, the layers of geogrids and geotextiles are almost intact. The test results of fatigue versus damage propagation rate lines are moving towards the bottom of the graphs for the non-reinforced condition, which means that reinforced specimens always have a lower propagation crack rate. This can be explained from the calculated values of B (crack propagation factor), which indicated that the rate of damage propagation in reinforced spec-

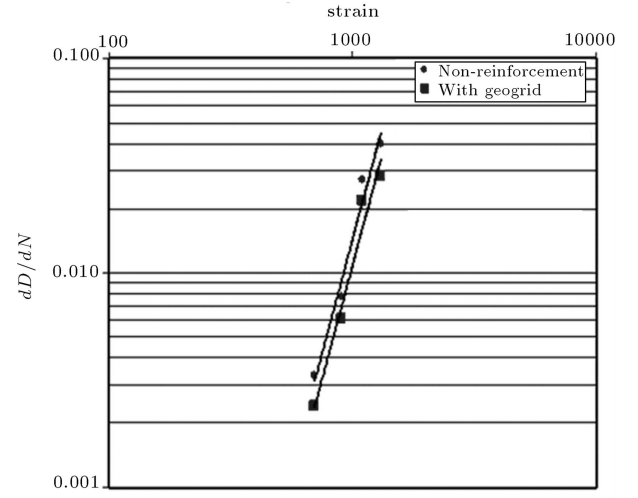


Figure 7. Comparison between damage propagation rate for non-reinforced specimen and that reinforced with geogrid.

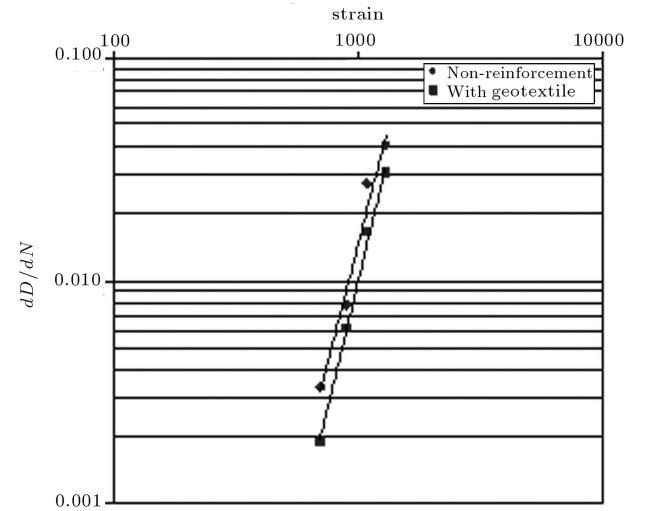


Figure 8. Comparison between damage propagation rate for reinforced specimen and for that reinforced with geotextile.

imens was lower than for the non-reinforced specimens. This reduction in rate is higher for specimens reinforced with geotextiles and lower strain levels and, also, for specimens reinforced with geogrid and higher strain levels.

According to the above statements, it can be concluded that geosynthetics delay the propagation and accumulation of primary micro cracks and, also, the development of macro cracks in asphalt pavements.

ACKNOWLEDGMENT

The authors would like to extend their appreciation to the Central Technical and Soil Mechanics Laboratory of the Road and Transportation Ministry for their

warm cooperation and permission to use their testing equipment.

REFERENCES

1. "Standard test method for determination of the fatigue life of compacted Hot Mix Asphalt (HMA) subjected to repeated flexural bending", *Standard Test AASHTO Provisional Standards*, TP8-94 (1994).
2. Saraf, C.L., Majidzadeh, K. and William, T. "Effect of reinforcement on fatigue life of asphalt beams", *Transportation Research Record*, N 1534, Nov, pp. 66-71 (2001).
3. Kim, K.W., Churl, Y.P. and Seok, Y.K. "Tensile reinforcement of asphalt concrete using polymer coating", *Construction and Building Materials*, **10**, pp. 141-146 (1996).
4. Holtz, R.D., Christopher, B.R. and Berg, R.R., *Geosynthetic Engineering*, BiTech Publishers Ltd., Canada (1997).
5. Industrial Fabric Association International (IFAI), a Design Primer "Geotextiles and related materials", Section 13, *Asphalt Overlay*, Industrial, Fabrics Association International, St. Paul, USA (1992).
6. Ingold, T.S. "The geotextiles and geomembrane, Manual", *Elsevier Advanced Technology*, UK (1994).
7. Indian Roads Congress (IRC), *Guidelines for Use of Geotextiles in Road, Pavements and Associated Works*, SP-59, India, Roads Congress, New Delhi, India (2002).
8. Ling, H.I. and Liu, Z. "Performance of geosynthetic-reinforced asphalt pavements", *Journal of Geotechnical and Geoenvironmental Engineering*, **127**(2), pp. 177-184 (2001).
9. Sprague, C.J. and Carver, C.A. "Asphalt overlay reinforcement", *Geotechnical Fabrics Report*, pp. 30-33 (2000).
10. Chang, T.T., Ho, N.H., Chang, H.Y. and Yeh, H.S. "Laboratory and case study for geogrid reinforced flexible pavement overlay", *TRB A2K07 Committee 78*, Annual Meeting (1999).
11. Perkins, S.W. "Geosynthetic reinforcement of flexible pavements: Laboratory based pavement test sections", *Federal Highway Administration Report FHWA/MT-99-001/8138*, Montana Department of Transportation (1999).
12. Kwasi, A. "In-situ behavior of geosynthetically stabilized flexible pavement", Thesis submitted to the Faculty of the Virginia Polytechnic Institute (1997).
13. Brown, S.F., Jones, C.P.D. and Broderick, B.V. "Use of non-woven fabrics in permanent road pavements", *Proceedings of the Institution of Civil Engineers*, London, UK, Part 2, **73**, pp. 541-563 (1982).
14. Hass, R., Wall, J. and Carroll, R.G. "Geogrid reinforcement of granular bases in flexible pavements", in *Transportation Research Record 1188*, TRB, National Research Council, Washington, DC, USA, pp. 19-27 (1988).
15. Barksdale, R.D., Brown, S.F. and Chan, F. "Potential benefits of geosynthetics in flexible pavement systems", *National Cooperative Highway Research Program Report* (1989).
16. Perkins, S.W. and Edens, M.Q. "A design model for geosynthetic-reinforced pavements", *The International Journal of Pavement Engineering*, **4**(1), pp. 37-50 (March 2003).
17. Rongzong, W. and Harvey, T.J. "Modeling of cracking in asphalt concrete with continuum damage mechanics", *16th ASCE Engineering Mechanics Conference July 16-18*, University of Washington, Seattle (2003).
18. Choi, Y.K., Collop, A.C. and Thom, N.H. "A simple damage approach to modeling fatigue in bituminous materials", *Bearing Capacity of Roads, Railways and Airfields*, pp. 103-11 (2002).
19. Ministry of Roads and Transportation, Research and Equation Center & Management and Planning Organization, Office of the Deputy for Technical Affairs, Technical Affairs and Standards Bureau, "Iran highway asphalt paving code", Issue No. 234 (2002).
20. Standard Test AASHTO Provisional Standards, "Standard test method for determination of the fatigue life of compacted Hot Mix Asphalt (HMA) subjected to repeated flexural bending", TP8-94 (1994).